Earth and Planetary Science Letters 279 (2009) 383–391

Contents lists available at ScienceDirect

Earth and Planetary Science Letters

journal homepage: www.elsevier.com/locate/epsl

Evaluating the role of microbial sulfate reduction in the early Archean using quadruple isotope systematics

Yanan Shen [a,*], James Farquhar [b,c], Andrew Masterson [b], Alan J. Kaufman [b], Roger Buick [d]

[a] CRC in Biogeochemistry, University of Quebec at Montreal, QC, Canada H3C 3P8
[b] Department of Geology and ESSIC, University of Maryland, College Park, MD 20742, USA
[c] Institute of Biology, Campusvej 55, University of Southern Denmark, 5230 Odense, Denmark
[d] Department of Earth & Space Sciences and Astrobiology Program, University of Washington, Seattle WA 98195-1310, USA

ARTICLE INFO

Article history:
Received 25 August 2008
Received in revised form 2 January 2009
Accepted 6 January 2009
Available online 15 February 2009

Editor: R.W. Carlson

Keywords:
sulfur isotopes
early Archean barite
microbial sulfate reduction
mass-independent
mass-dependent

ABSTRACT

Microscopic pyrites with low $^{34}S/^{32}S$ ratios in ~3.47-Gyr-old sedimentary barites from North Pole, Australia have been interpreted as evidence for microbial sulfate reduction and/or sulfur disproportionation in the early Archean. We show that these microscopic sulfides have similar to slightly less negative $\Delta^{33}S$ and slightly more negative $\Delta^{36}S$ values compared to the enclosing sulfate crystals. This finding is consistent with a primary mass-independent signature overprinted by biological sulfate reduction, as calibrated by previous experimental laboratory culture studies. However, it is inconsistent with an overprint by abiological sulfate reduction or sulfur disproportionation, as predicted by isotope exchange theory and laboratory culture studies. Thus, our multiple sulfur isotope measurements support the contention that sulfate-reducing microbes had evolved by ~3.47 billion years ago.

1. Introduction

Microbial sulfate reduction is an energy-yielding metabolic process during which sulfate is reduced and sulfide is produced coupled with the oxidation of organic matter or H_2 (e.g., $SO_4^{2-} + CH_3COO^- + H_2O \rightarrow H_2S + 2HCO_3^- + OH^-$) (Postgate, 1984). Experiments with pure cultures and natural populations of sulfate-reducing microbes have demonstrated that sulfides are enriched in ^{32}S with fractionations ($\approx \delta^{34}S_{sulfate} - \delta^{34}S_{sulfide}$) of 2–46‰ (Chambers and Trudinger, 1979; Bolliger et al., 2001; Detmers et al., 2001), but more typically between 10 and 40‰ (Habicht and Canfield, 1997; Canfield, 2001) relative to parent sulfate when it is abundant. In nature, sulfides produced during microbial sulfate reduction mostly react with metal ions, especially Fe, and largely precipitate as pyrite (FeS_2) (Berner, 1984; Wilkin and Barnes, 1996; Rickard, 1997). Because no certain cellular remains of sulfate reducing microbes or their biomarker molecules have been identified in the ancient rock record, understanding the early evolution of microbial sulfate reduction depends critically on sulfur isotopic measurements of sulfate and pyrite in sedimentary rocks (Shen and Buick, 2004), where large fractionations between pyrite and seawater sulfate measured from geological samples have been regarded as diagnostic of microbial sulfate reduction (Schidlowski et al., 1983).

The antiquity of sulfur metabolisms has been explored using sulfur isotope fractionations, with the earliest evidence reported from rocks of the ~3.47 Gyr Dresser Formation from North Pole, northwestern Australia. Here, microscopic pyrite grains aligned along the growth faces of barite crystals show a wide range of $\delta^{34}S$ values with large fractionations, greater than 20‰, relative to co-existing sulfate. These large fractionations and the geologic, petrographic, and mineralogic context led to the suggestion that Dresser Formation depositional environments harbored microbial sulfate reducers (Shen et al., 2001).

A recent ion microprobe study documented positive $\Delta^{33}S$ and negative $\delta^{34}S$ in microscopic sulfides from Dresser Formation barites that have been used to argue that a second metabolism, sulfur disproportionation, was instead operating at ~3.47 Ga (Philippot et al., 2007). Positive $\Delta^{33}S$ is considered to be a signature of the Archean elemental sulfur pool and is distinct from the negative $\Delta^{33}S$ inferred for the Archean sulfate pool (Farquhar et al., 2000, 2001). Disproportionation of sulfur compounds of intermediate redox state to sulfide and sulfate also produces large fractionations (approaching 60‰ for $\delta^{34}S$) and the impact of microbial sulfur disproportionation on the geological sulfur isotope record is thought to have been significant during younger times in Earth history (Canfield and Teske,

* Corresponding author.
E-mail address: shen.yanan@uqam.ca (Y. Shen).

0012-821X/$ – see front matter © 2009 Elsevier B.V. All rights reserved.
doi:10.1016/j.epsl.2009.01.018

1996; Johnston et al., 2005b). The suggestion by Philippot et al. (2007) may thus carry implications for the activity of sulfur disproportionation ~3.47 billion years ago.

These two biogenic interpretations of the Dresser Formation isotopic record contrast with a proposal that the variations for $\delta^{34}S$ instead reflect purely abiological processing of sulfur in a hydrothermal (Runnegar et al., 2001) or atmospheric (Mojzsis, 2006) setting. On its own, $^{34}S/^{32}S$ data does not provide a straightforward way to distinguish between these sulfur-cycling pathways, but recent progress in understanding the metabolic transformations of sulfur using all four stable sulfur isotopes (Johnston et al., 2007) provides a new way to approach this question.

2. Early Archean barite (~3.47 billion years old) at North Pole, northwestern Australia

The samples examined here come from previous $\delta^{34}S$ studies of Dresser Formation microscopic sulfides (Shen et al., 2001; Philippot et al., 2007) and from new collections (Table 1). Previous petrographic studies of the North Pole locality indicate that the samples have only been subjected to low-strain brittle deformation and prehnite–pumpellyite to lowermost greenschist facies metamorphism (Dunlop and Buick, 1981). Original sedimentary minerals were replaced by chert and barite during hydrothermal alteration, but textures and structures preserved in the chert and surrounding basalt indicate that the depositional environment was shallow marine to intermittently exposed, e.g. wave ripples, desiccation breccias, well-sorted tidal cross-beds and scoriaceous tops to pillowed basalt flows (Groves et al., 1981). Primary sulfate deposits have been interpreted to have formed in back-barrier lagoons separated from the ocean by beach bars of rafted pumice (Buick and Barnes, 1984; Buick and Dunlop, 1990). These were surrounded by tidal flats composed of carbonate sand or volcanogenic mud, in both of which diagenetic sulfate crystals and nodules precipitated. Both types of sulfate grew before lithification, indicated by broken primary sulfate crystals rounded by sedimentary transport and by cores of incorporated sediment in diagenetic crystals (Buick and Dunlop, 1990). Sometimes cryptically cross-cutting dykes and sills of secondary barite and of pyritic black chert disrupt the sedimentary succession, filling brittle fractures and faults that formed after sediment lithification (Buick and Dunlop, 1990).

Table 1
The early Archean barite (~3.47 billion years old) at North Pole, Northwestern Australia

Sample no.	Description
NP 89	Uppermost bed of bedded barite with bladed crystals draped by silicified tuffaceous arenite, B deposit mine (1:50,000 North Pole topographic map sheet 2755-1, AMG co-ordinates 075294, 765894).
NP 124	Bedded barite overlain by massive grey chert with rhombic carbonate inclusions; from section J in (Buick, R., 1985. Life and conditions in the early Archaean: evidence from 3500 m.y. old shallow-water sediments in the Warrawoona Group, North Pole, Western Australia. Ph.D. thesis, University of Western Australia, 353 pp.), 7.79 m stratigraphic height (075383, 766416)
21016	Vein barite immediately beneath bedded barite (075381, 766425)
21019	Basal bedded barite, 0.00 m from base of barite unit (075383, 766386)
21021	Bedded barite immediately below bed of silicified gypsiferous peloidal tuff-carbonate arenite, 1.59 m from base of barite unit (075383, 766386)
21022	Bedded barite immediately above bed of silicified gypsiferous peloidal tuff-carbonate arenite, 2.06 m from base of barite unit (075383, 766386)
21025	Bedded barite from upper unit, 3.82 m from base of barite unit (075383, 766386)
21026	Bedded barite from upper unit, 4.01 m from base of barite unit (075383, 766386)
21028	Vein barite at base of vein containing 21016 (075397, 766349)
21029	Vein barite near Breens copper deposit (074682, 766495)
21031	Bedded barite, B deposit mine (075294, 765894)
GIS 95.0	Macroscopic sulfide laminate (drill core: 2C)
GIS 96.6	Microscopic sulfide (drill core: 2C)
GIS 96.7	Microscopic sulfide (drill core: 2C)

Primary sulfate crystals form lenticular beds up to 0.5 km in lateral extent and up to 10 m thick. Individual layers of sulfate crystals, now dark grey barite, are up to 15 cm thick, composed of bottom-nucleated fans of bladed hemipyramids (Buick and Dunlop, 1990). Usually, bedded barite layers are separated by thin (~1 cm) wavy partings of iron oxides which, where freshly exposed, are composed of pyrite. As well, individual barite crystals contain sulfidic micro-inclusions, mostly pyrite, aligned along growth faces of the original crystals. This textural relationship indicates the syngeneity of sulfate and sulfide minerals. The microscopic pyrites are ~50 μm in size, comprise less than 1% of the rock and are closely associated with kerogen inclusions (Buick and Dunlop, 1990).

Interfacial angle measurements on both primary and diagenetic sulfate crystals using a universal-stage microscope (Lambert et al., 1978; Buick and Dunlop, 1990) show that at least some of both crystal types were initially composed of gypsum ($CaSO_4{\cdot}2H_2O$), according to the Law of Constancy of Interfacial Angles (Steno, 1669). Barite replacement of gypsum evidently occurred soon after deposition, shown by the perfect preservation of crystal morphologies of the highly soluble gypsum. Subsequently, all sulfate crystals underwent silicification to a depth of several millimetres, penetrating marginally to cleavage planes of the barite in primary sulfates but completely or almost completely silicifying the small diagenetic gypsum crystals (Buick and Dunlop, 1990). It should be noted that several of the isotopic analyses reported here (NP 89) come from a sample from the same sediment-draped barite lamina from the same locality as the interfacial angle measurements showing that the barite is pseudomorphous after gypsum. Notably, barite crystals in the cross-cutting dykes and sills display typical orthorhombic barite morphologies and show no evidence of gypsum precursors.

It has been proposed that, rather than a marginal marine depositional environment with evaporitic gypsum precipitation, the Dresser Formation sulfate was initially precipitated as barite, not gypsum, by hydrothermal processes (Runnegar et al., 2001) in a felsic volcanic caldera (Nijman et al., 1998; van Kranendonk, 2006). In this model, the evidence that sulfate originally precipitated as barite came from X-ray computerized tomography (X-ray CT) (Runnegar, 2000). However, X-ray CT only images density contrasts in the sample, so this technique cannot reveal original crystal morphology in partially silicified sediments where the microquartz–barite boundary is within the original crystal boundary along barite cleavage planes. By contrast, the universal-stage petrographic technique used in previous studies (Lambert et al., 1978; Buick and Dunlop, 1990) differentiates between the inclusion-rich microquartz of the surrounding silicified sediment and the inclusion-poor microquartz of the silicifed sulfate crystals, thus yielding accurate interfacial angle measurements. Moreover, no felsic lavas occur within the purely basaltic volcanic succession beneath the Dresser Formation at North Pole, and felsic tuffs are insignificant compared with mafic ash within the formation (Dunlop and Buick, 1981; Groves et al., 1981; Buick and Barnes, 1984), thus providing no support for a felsic caldera depositional setting. The low-temperature origin of the precursor gypsum (<58 °C in pure water (Hardie, 1967) ranging down to <18 °C at halite saturation (Blount and Dickson, 1973) conflicts with a hydrothermal origin for the sulfate, as does the consistently positive barite $\delta^{34}S$ values of +4 to +5‰ (Lambert et al., 1978; Shen et al., 2001; Runnegar et al., 2001; Philippot et al., 2007), which differ markedly from that precipitated in either high-sulfidation magmatic or low-sulfidation meteoric hydrothermal mineralizing systems in felsic settings (Rye, 2005). Lastly, a solely juvenile hydrothermal sulfate source is precluded by evidence for mass-independent sulfur isotope fractionation (Runnegar et al., 2001; Philippot et al., 2007), a phenomenon only known to reflect an atmospheric source (Farquhar et al., 2000; Farquhar and Wing, 2003).

3. Analytical methods

Pyrite sulfur from barite samples was extracted with a chromium reduction solution and converted to silver sulfide (Canfield et al.,

Table 2
The S-isotopic values of coexisting pyrite and sulfate in the North Pole barite deposit

	$\delta^{33}S$	$\delta^{34}S$	$\delta^{36}S$	$\Delta^{33}S$	$\Delta^{36}S$	$\delta^{34}S_{sulfate}$	$\delta^{34}S_{sulfate}-\delta^{34}S_{sulfide}$	$\Delta^{33}S+\Delta^{36}S$
Pyrites								
YS-NP124-new extraction	−4.587	−7.763	−15.57	−0.582	−0.87	8.7	16.5	−1.45
NP-124-sample from S01	−1.654	−3.252	−7.44	0.022	−1.27	8.7	12.0	−1.25
YS-NP-89-new extraction	−11.400	−19.686	−36.58	−1.213	0.49	4.3	24.0	−0.73
NP-89-sample from S01	−9.486	−16.060	−25.54	−1.183				
GIS 95.0 II macroscopic	−0.861	−1.254	−2.53	−0.215	−0.15	5.0	6.3	−0.37
GIS 96.6 II microscopic	−1.243	−1.849	−3.77	−0.290	−0.26	5.0	6.8	−0.55
GIS 96.7 II microscopic	−2.772	−4.730	−8.71	−0.333	0.26	5.0	9.7	−0.08
NP21019A-Py	−2.888	−4.696	−8.64	−0.467	0.26	5.0	9.7	−0.21
NP21019B-Py	−3.752	−6.315	−11.44	−0.495	0.52	4.8	11.1	0.03
NP21019C-Py	−3.312	−5.613	−10.25	−0.418	0.39	5.7	11.3	−0.03
NP21021-Py	−5.020	−8.465	−15.63	−0.652	0.40	5.0	13.5	−0.26
NP21022A-Py	−6.196	−10.442	−18.82	−0.805	0.93	5.3	15.7	0.12
NP21025-Py	−4.840	−8.087	−14.86	−0.667	0.45	4.8	12.9	−0.22
NP21026-Py	−5.614	−9.575	−18.10	−0.671	0.01	5.0	14.6	−0.66
NP21031-Py	−4.391	−7.155	−12.93	−0.699	0.62	4.2	11.4	−0.08
NP21016-Py	−7.508	−12.929	−22.77	−0.829				
NP21029-Py	−6.612	−10.349	−18.27	−1.269	1.31	5.0	15.3	0.04
Barite								
NP21016-SO_4	0.997	4.159	9.38	−1.143	1.46		0.8	0.32
NP21019B-SO_4	1.470	4.839	10.39	−1.019	1.17		0.2	0.15
NP21019C-SO_4	1.950	5.689	11.64	−0.976	0.80		−0.7	−0.17
NP21022A-SO_4	1.505	5.289	11.34	−1.215	1.27		−0.3	0.05
NP21025-SO_4	1.171	4.793	10.40	−1.295	1.27		0.2	−0.02
NP21028-SO_4	0.890	4.275	9.48	−1.309	1.34		0.7	0.03
NP21031-SO_4	0.854	4.212	9.24	−1.313	1.22		0.8	−0.09

$\delta^{34}S$ of +5‰ for sulfate was used to calculate fractionations ($\delta^{34}S_{sulfate}-\delta^{34}S_{sulfide}$) for the samples without measured $\delta^{34}S$ values. For other samples, the measured $\delta^{34}S$ values for sulfate were used.

1986). Tests undertaken using various forms of sulfate provided no evidence that sulfate sulfur was extracted and precipitated as silver sulfide during the Cr-reduction process. Residual sulfate after Cr-reduction was reacted with a heated solution consisting of a 3.3:2:1 mixture of 12 *N* hydrochloric, 48% hydroiodic, and 50% hypophosphorous acids using an apparatus described by Forrest and Newman (1977). During this procedure, sulfate was reduced to H_2S by heating the solution to just below its boiling point for 3 h. The product H_2S was carried by nitrogen gas through a condenser and a bubbler filled with milli-Q water, and collected as zinc sulfide by reaction with a slightly acidic Zn-acetate solution. The zinc sulfide was reacted with silver nitrate to yield silver sulfide, which was collected centrifugation and

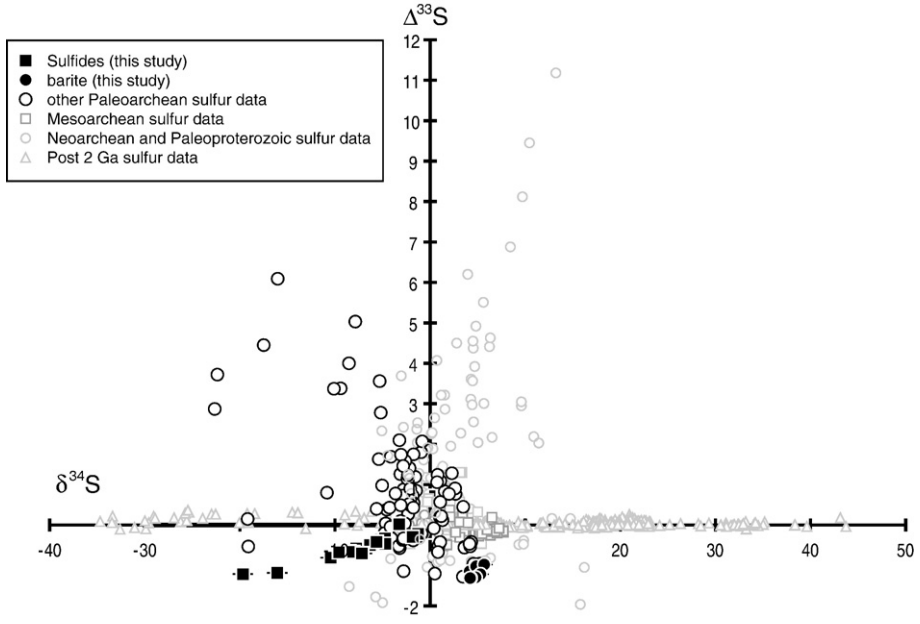

Fig. 1. Plot of $\Delta^{33}S$ vs. $\delta^{34}S$ for North Pole samples and for other samples from the geological record. Plotted here are data for North Pole sulfate analyzed here (black filled circular symbols), sulfide (black filled square symbols). Plotted data also included from other Paleoarchean samples (black unfilled symbols), Mesoarchean samples (grey unfilled squares), Neoarchean (grey unfilled circles) and samples younger than 2 Gya (grey unfilled triangles). Data from Johnston et al. (2006), Ono et al. (2003), Mojzsis et al. (2003), Papineau et al. (2007), Kamber and Whitehouse (2007), Bekker et al. (2004), Ohmoto et al. (2006), Philippot et al. (2007), Bao et al. (2007), Farquhar et al. (2000, 2002, 2007a) and Kaufman et al. (2007). Error bars are estimates of 2 sigma uncertainties.

washed with successive rinses of milli-Q water, ammonium hydroxide solution, and milli-Q water.

Silver sulfide (Ag_2S) was converted to SF_6 by fluorination by reaction with a 5-fold excess of F_2 at 250 °C for 8 h in a Ni reaction vessel. After the reaction, product SF_6 was condensed from the residual F_2 into a liquid-nitrogen cooled trap (−177 °C). The F_2 was transferred to another part of the manifold where it was passivated by reaction with hot KBr. The SF_6 was subsequently thawed to room temperature, and then cooled to −111 °C to condense contaminants such as trace HF, before it was transferred to the injection loop of a gas chromatograph (GC) cooled to −177 °C. GC purification of SF_6 was undertaken using a composite column consisting of a 1/8 in. diameter, six foot lead column of 5A molecular sieve, followed by a 1/8 in. diameter, 12 ft long Haysep-Q™ column. The He carrier flow was set at 20 mL/min. The SF_6 peak was registered on a TCD and then isolated by freezing into a liquid-nitrogen cooled trap. The isotopic composition of the purified SF_6 was determined by dual-inlet gas-source mass spectrometry monitoring ion beams at *m*/*e* of 127, 128, 129, and 131 using a Thermo Finnigan MAT 253 gas source mass spectrometer.

Sulfur isotope data are presented using standard notation ($\delta^{34}S$, $\Delta^{33}S$ and $\Delta^{36}S$) where $\Delta^{33}S = \delta^{33}S - 1000 \times ((1+\delta^{34}S/1000)^{0.515} - 1)$ and $\Delta^{36}S = \delta^{36}S - 1000 \times ((1+\delta^{34}S/1000)^{1.90} - 1)$. $\Delta^{33}S$ and $\Delta^{36}S$ describe the deviation of a sample datum from a reference mass-dependent fractionation line. One sigma uncertainties for samples near the mass-dependent fractionation line are estimated on the basis of repeat analyses of reference materials to be better than ±0.2‰, ±0.01‰, and ±0.2‰ in $\delta^{34}S$, $\Delta^{33}S$ and $\Delta^{36}S$, respectively. Uncertainties on samples with large mass-independent fractionations may be larger than these estimates. The results of our measurements are presented in Table 2. Data are presented relative to V-CDT with an assigned value relative to IAEA S-1 having $\delta^{34}S = -0.3$‰, $\Delta^{33}S = 0.0944$‰, and $\Delta^{36}S = -0.69$‰.

4. Results

Our analyses of all four stable isotopes for barite and pyrite within the barite crystal fans showed uniformly negative $\Delta^{33}S$ and did not resolve the population of positive $\Delta^{33}S$ values of microscopic pyrite identified by secondary ion mass spectrometry (Philippot et al., 2007). $\delta^{34}S$ values ranged from +5.7 to +4.2‰ for sulfates and from −1.3 to −19.7‰ for microscopic pyrites. $\Delta^{33}S$ values ranged from −0.98 to −1.31‰ for sulfates and from +0.02 to −1.27‰ for microscopic pyrites. $\Delta^{36}S$ values ranged from +0.8 to +1.5‰ for sulfates and −1.3 to +1.3‰ for microscopic pyrites (Table 2).

While the sulfur isotope compositions for the barite were quite homogenous ($\delta^{34}S = +4.75 \pm 0.58$‰, $\Delta^{33}S = -1.18 \pm 0.14$‰, and $\Delta^{36}S = +1.22 \pm 0.21$‰; mean ± 2σ std. deviation), the sulfur isotope compositions for the pyrite exhibited systematic covariation between $\Delta^{33}S$ values and $\delta^{34}S$ values (Fig. 1). The pyrite data form an array that extends from $\Delta^{33}S = +0.02$‰ and $\delta^{34}S = -1.3$‰ to $\Delta^{33}S = -1.27$‰ and $\delta^{34}S = -19.7$‰. One population falls to the left of and below the field of data defined by all Archean data (Fig. 2), yielding a different $\Delta^{36}S/\Delta^{33}S$ array. A regression through the entire dataset yields $\Delta^{36}S = -1.51 \cdot \Delta^{33}S - 0.64$, which is inconsistent with the slope of the arrays defined by Paleoarchean and Neoarchaean datasets (cf., Farquhar et al., 2000; Kaufman et al., 2007). The slope of this array is not inconsistent with the slopes of arrays derived from some Mesoarchean data (Farquhar et al., 2007a), but none of the data from these Mesoarchean successions exhibits the same internal variability with respect to $\Delta^{33}S$ and $\delta^{34}S$, and $\Delta^{36}S$ and $\Delta^{33}S$ of pyrite from the North Pole sample set.

5. Discussion

The observation of more than one generation of sulfide (as identified by multiple sulfur isotope ratios) in Archean age samples is not unique.

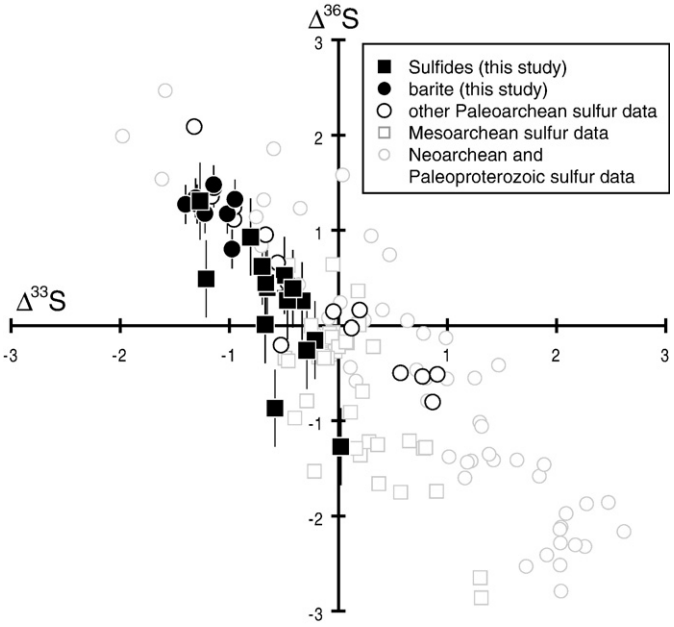

Fig. 2. Plot of $\Delta^{36}S$ vs. $\Delta^{33}S$ for sulfate (black filled circular symbols) and sulfide (black filled square symbols). Plotted data also included from other Paleoarchean samples (black unfilled symbols), Mesoarchearn samples (grey unfilled squares), and Neoarchean (grey unfilled circles). Data from Farquhar et al. (2000, 2007a) and Kaufman et al. (2007). Error bars are estimates of 2 sigma uncertainties.

For instance Kamber and Whitehouse (2007) have documented large isotopic variations for samples from the late Archean Gamohaan Formation. The origin of these variations is unclear, but it has been hypothesized that sulfide with positive $\Delta^{33}S$ was produced in a different part of the mineralizing system from a different sulfur source than that with negative $\Delta^{33}S$. A recent SIMS study by Fike et al. (2008) reports large variations in $\delta^{34}S$ between modern microenvironments that would not be observed by bulk techniques, further illustrating the potential for highly localized sulfur isotope heterogeneities.

We can think of two general interpretations that can explain the sulfur isotope variations for these North Pole samples. The variation in $\Delta^{33}S$ and $\Delta^{36}S$ could result from varying the source reactions causing initial mass-independent fractionation, implying that changes in these source reactions reflected changes in atmospheric chemistry and possibly composition. Alternatively, the variation in $\delta^{34}S$, $\Delta^{33}S$ and $\Delta^{36}S$ could result from a combination of mass-dependent and mass-independent isotope effects, as suggested by Ueno et al. (2006).

The case for a change in atmospheric source reactions has been argued for other Archean sequences (e.g., Farquhar et al., 2007a; Kaufman et al., 2007) on the basis of observed changes in the relationships between $\Delta^{36}S$ and $\Delta^{33}S$ for narrow intervals in the geologic record. Kaufman et al. (2007) reported differences in the relationship between $\Delta^{36}S$ and $\Delta^{33}S$ between the upper and lower parts of the Neoarchean Mt. McRae Shale in northwest Australia and suggested that these variations may reflect changes in atmospheric composition. Farquhar et al. (2007a) reported differences in $\Delta^{36}S$ and $\Delta^{33}S$ relationships at the formation level for Mesoarchean samples and suggested that these may be related to variations in atmospheric composition or in the ultraviolet radiation transmitted through the atmosphere. Interpretations in both of these studies were made on the basis that the isotope systematics appeared to be coherent at the formation level, or at least for significant intervals within formations. At North Pole, we do not see a coherent relationship between $\Delta^{36}S$ and $\Delta^{33}S$ but do observe a significant correlation of $\Delta^{33}S$ with $\delta^{34}S$, so the alternative interpretation of a mass-dependent process overprinting onto a singular (or nearly singular) mass-independent array may prove a more parsimonious

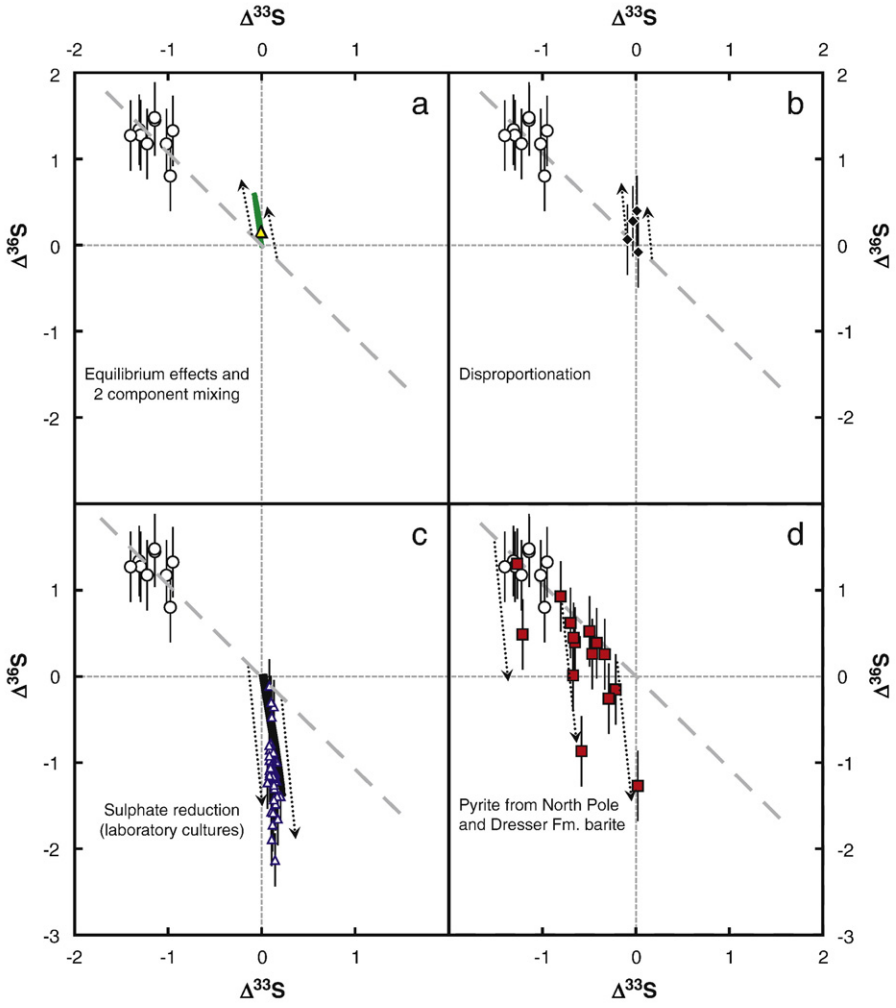

Fig. 3. Plots of $\Delta^{36}S$ vs $\Delta^{33}S$. Unfilled circles are measurements of North Pole barite. Dashed grey line is $\Delta^{36}S=-\Delta^{33}S$ and represents approximation of a reference mass-independent fractionation array. Grey dotted lines indicate principal axes of plots. Vectors (dotted black lines with arrowheads) illustrate deviation from the mass-independent fractionation array for sulfide relative to sulfate that is related by (a) equilibrium isotope fractionation (yellow filled triangles) and two component mixing with sulfate (green line), (b) sulfur disproportionation (black diamonds) observed in laboratory culture experiments (Johnston et al., 2005a; 2007), (c) sulfate reduction as observed (blue triangles) in laboratory culture experiments (Farquhar et al., 2003a; Johnston et al., 2005a; 2007) and as predicted by network models (black line) experiments (Johnston et al., 2007; Farquhar et al., 2007b), and (d) pyrite from North Pole reported here (red filled squares). Error bars are estimates of 2 sigma uncertainties.

explanation for the isotopic variability. This suggestion is also in line with previous studies that suggested that correlations between $\delta^{34}S$ and $\Delta^{33}S$ for pyrites reflect mixing of a mass-dependently fractionated sulfur pool with negative $\delta^{34}S$ and $\Delta^{33}S$ derived from sulfate reduction with a mass-independently fractionated sulfur pool with positive $\delta^{34}S$ and $\Delta^{33}S$ (e.g., Ono et al., 2003).

Fig. 1 illustrates the relationship between $\delta^{34}S$ and $\Delta^{33}S$ in our North Pole pyrite and barite samples. For the pyrites, we interpret this relationship to be consistent with a mixing array. One end member of this array would have positive $\delta^{34}S$ and $\Delta^{33}S$ and the other would have negative $\delta^{34}S$ of at least −19.7‰ and negative $\Delta^{33}S$ of at least −1.27‰. This composition is broadly consistent with mass-dependent $^{34}S/^{32}S$ fractionation of approximately 25‰ relative to North Pole barite sulfate ($\delta^{34}S$ ~+5‰). A question thus arises about its origin because a fractionation of 25‰ for $\delta^{34}S$ could arise from almost any of the processes that have been proposed for this locality—hydrothermal equilibrium isotope effects (e.g., Runnegar et al., 2001), microbial sulfate reduction (Shen et al., 2001), or microbial sulfur disproportionation (Philippot et al., 2007). Our goal is to see if we can use what is known about the sulfur isotopic fractionations $\delta^{34}S$, $\Delta^{33}S$ and $\Delta^{36}S$ produced by these different processes to provide additional constraints on the origin of the barite at North Pole and Paleoarchean sulfur cycling.

5.1. Mass-dependent sulfur isotope effects (fractionations)

Theoretical calculations have been used to describe a variety of relevant equilibrium isotope effects (e.g., Ono et al., 2006; Farquhar et al., 2007b; Johnston et al., 2007; Otake et al., 2008), and these show that variations for $\Delta^{33}S$ and $\Delta^{36}S$ will be small (less than ~±0.03‰ for $\Delta^{33}S$ and less than ~±0.3‰ for $\Delta^{36}S$) under most natural conditions. These include the types of effects that occur during hydrothermal reduction processes (e.g., Runnegar et al., 2001) and hydrothermal disproportionation reactions.

Experiments with pure cultures of sulfate reducing microbes have yielded slightly larger variations for $\Delta^{33}S$ and $\Delta^{36}S$ ($\Delta^{33}S$ ranging from ~+0.06 to ~+0.20‰ and $\Delta^{36}S$ ranging from ~−0.3 to ~−2.1‰ for product sulfide relative to reactant sulfate) (Johnston et al., 2007). These variations are correlated with $\delta^{34}S$ and their origin has been attributed to the mixing of sulfur during the metabolic transformations that result in its reduction. Quantitative treatments that reconcile the observations made in these and other experiments with published metabolic models are presented in Farquhar et al. (2003, 2007b, 2008) and in Johnston et al. (2007).

Studies of $\delta^{34}S$, $\Delta^{33}S$ and $\Delta^{36}S$ for products from laboratory experiments with sulfur disproportionating microbes that metabolize

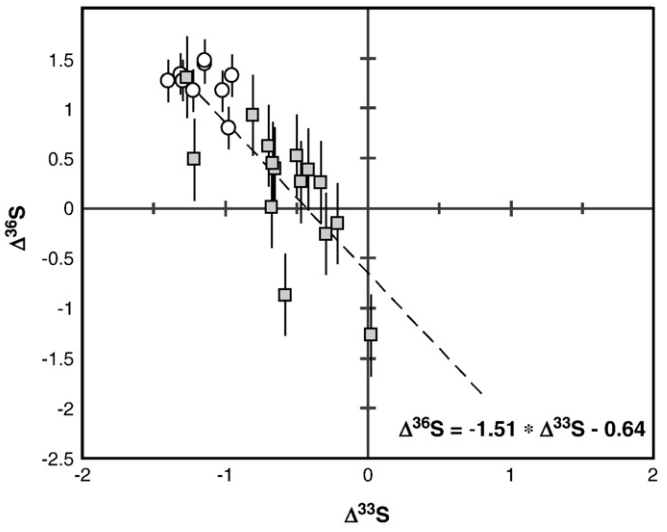

Fig. 4. Plot of $\Delta^{36}S$ vs. $\Delta^{33}S$ for sulfate (white circular symbols) and sulfide (filled square symbols). Line on plot is regressed and is described by the equation $\Delta^{36}S = -1.51 \cdot \Delta^{33}S - 0.64$. Error bars are estimates of 2 sigma uncertainties.

elemental sulfur and sulfite have been reported by Johnston et al. (2005a, 2007). These studies have documented sulfide with $\Delta^{33}S$ ranging from ~+0.03 to ~−0.09‰ and $\Delta^{36}S$ ranging from ~+0.5 to ~−0.1‰ for product sulfide relative to reactant sulfate.

Thus, the three different types of mass-dependent processes proposed as explanations for the isotope systematics at North Pole should result in differing behaviors of $\delta^{34}S$, $\Delta^{33}S$, and $\Delta^{36}S$. Using such logic, it should also be possible to test whether mixing calculations involving mass-independently fractionated precursor sulfur pools *and* sulfide produced by reduction from a precursor sulfate pool by each of these three processes can provide a self consistent explanation for the data.

Our isotopic data show that the $\Delta^{33}S$ for disseminated microscopic pyrites is always less negative than the corresponding $\Delta^{33}S$ of matrix barite sulfate, with a difference ranging from 0.31‰ to 0.63‰. We view this as an indication that the pyrite sulfur and sulfate sulfur are not directly related by a single step mass-dependent isotope effect or by a simple discrimination of isotopes, but show mixing between sulfur fractionated by mass-dependent and mass-independent processes. The isotope mixing calculations presented below are designed to see through the effects of such mixing, as are the projections that collapse a 3-D framework defined by $\delta^{34}S$, $\Delta^{33}S$ and $\Delta^{36}S$ onto two dimensional plots.

5.2. Sulfur isotope mixing calculations

We present the results of our mixing calculations in Figs. 3–5. These plots illustrate the nature of predicted co-variation of $\Delta^{36}S$ with $\Delta^{33}S$ (Fig. 3), and the covariation between $\Delta^{36}S$ and the magnitude of the mass-dependent fractionation between sulfide and sulfate in terms of $\delta^{34}S$ (Figs. 4 and 5).

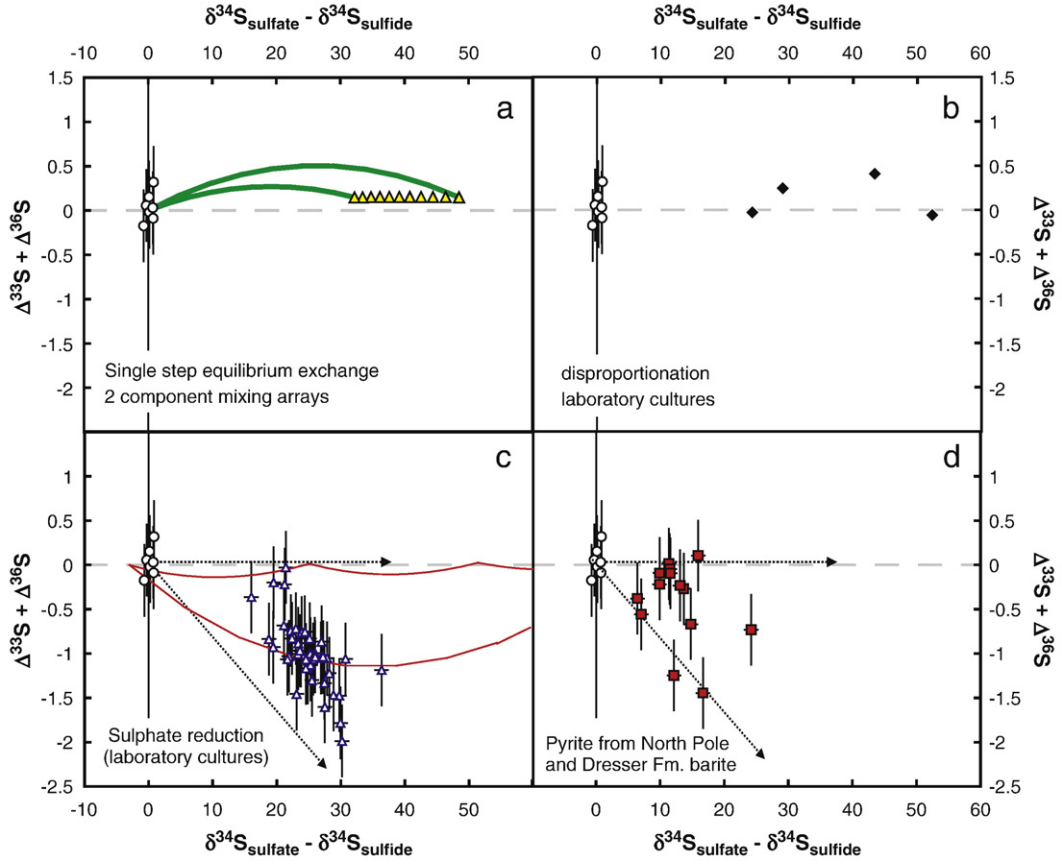

Fig. 5. Plot of the deviation of from the reference mass-independent fractionation array ($\Delta^{36}S+\Delta^{33}S$) (from Fig. 1 $-\Delta^{36}S=-\Delta^{33}S$) versus the isotopic fractionation of $^{34}S/^{32}S$ between sulfate and sulfide ($\delta^{34}S_{sulfate}-\delta^{34}S_{sulfide}$). Unfilled circles are measurements of North Pole barite referenced to estimated average composition for sulfate). Dashed grey line is $\Delta^{36}S=-\Delta^{33}S$ and represents approximation of a reference mass-independent fractionation array. Plots for (5a) equilibrium isotope fractionation (yellow filled triangles) and two component mixing with sulfate (green curves), (5b) sulfur disproportion observed in laboratory culture experiments (Johnston et al., 2005a; 2007) (black diamonds), (5c) sulfate reduction as observed in laboratory culture experiments (Farquhar et al., 2003a; Johnston et al., 2005a; 2007) (blue unfilled triangles) and as predicted by network models (Johnston et al., 2007; Farquhar et al., 2007b) (red lines) and (5d) pyrite from North Pole reported here (red filled squares). Vectors (dotted lines with arrowheads) in 5c and 5d illustrate the direction and limits of deviation from the mass-independent fractionation array for sulfide relative to sulfate that is found in experiments with cultures of microbial sulfate reducers. Error bars are estimates of 2 sigma uncertainties.

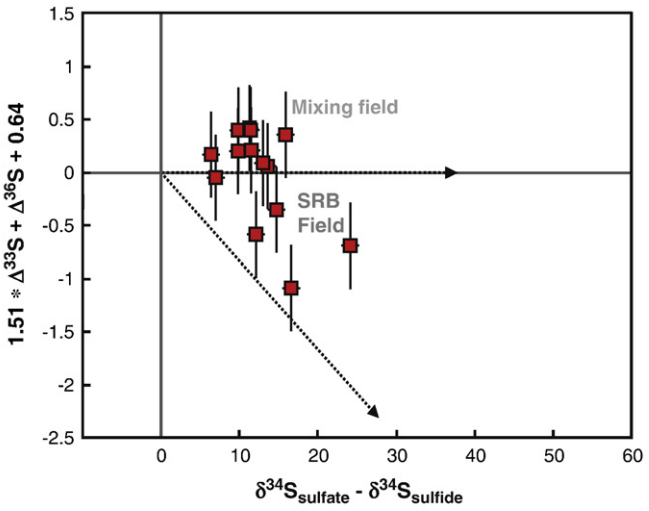

Fig. 6. Plot of $\Delta^{36}S+1.51\cdot\Delta^{33}S+0.64$ vs. the isotopic fractionation between sulfate and sulfide ($\delta^{34}S_{sulfate}-\delta^{34}S_{sulfide}$). The dotted arrows on this plot are the same as those in Fig. 4 and describe the field of data predicted for dissimilatory sulfate reducers on the basis of laboratory experiments. Error bars are estimated at the 2 sigma level.

Fig. 3 illustrates three cases. In this figure we assume that the precursor mass-independently fractionated sulfur pools lie on a single array with a slope of −1 (i.e. $\Delta^{36}S\approx-\Delta^{33}S$). We note that in reality this array may vary, but the general features of the illustration will still hold. The data from the North Pole barite lie on this array.

Case 1 (Fig. 3a) illustrates the composition of sulfide in equilibrium with sulfate having $\Delta^{36}S=0$ and $\Delta^{33}S=0$ at temperatures of ~100–200 °C, and the two-component mixing of this sulfide with juvenile sulfur. If this calculation were done for sulfide formed from sulfate having a different $\Delta^{36}S$ and $\Delta^{33}S$, the array that would be predicted would originate at the point defined by this composition and also rise to slightly more positive $\Delta^{36}S$. Hence, whatever the starting composition, sulfide produced by equilibrium hydrothermal reduction of sulfate would have small ^{36}S *enrichments* relative to the mass-independent fractionation array and would not define a field that overlapped with our North Pole data.

Case 2 is illustrated in Fig. 3b and presents a mixing calculation for sulfide normalized to sulfate that would lie on the same mass-independent array with $\Delta^{36}S=0$, $\Delta^{33}S=0$. Case 2 uses information derived from laboratory culture experiments with sulfur disproportionators (Johnston et al., 2005a, 2007). This calculation also produces mixing products that have slightly more positive $\Delta^{36}S$ and small ^{36}S *enrichments* relative to the mass-independent fractionation array, similarly failing to define a field that overlapped with our data.

Case 3 is illustrated in Fig. 3c. This figure presents a mixing calculation for the sulfide produced in laboratory culture experiments with sulfate reducers. It also assumes a precursor sulfate that lies on the mass-independent array with $\Delta^{36}S=0$, $\Delta^{33}S=0$. The consequence of mixing sulfide produced by microbial sulfate reduction with sulfide that lies on the inferred mass-independent array for precursor sulfur species is a shift to more negative $\Delta^{36}S$ without significant change in $\Delta^{33}S$. This same shift would also be observed if the source sulfate has more negative $\Delta^{33}S$ such as is observed in the North Pole barites. The field defined by this calculation overlaps the field occupied by the data from North Pole (Fig. 3d).

If the precursor sulfur pools followed another relationship, such as the one provided by the regression through the data (i.e. $\Delta^{36}S=-1.51\cdot\Delta^{33}S-0.64$, as described above: Fig. 4), a number of the points that lie above this regression line could be accounted for by the hydrothermal (equilibrium) and disproportionation models, but these points would still fall within error of the field defined by the model with microbial sulfate reduction. The few points that are most ^{36}S *depleted* would fall within the field defined by the model with microbial sulfate reduction, but *not* the fields defined by the other processes. We note that the mass-independent array described by this equation does not pass through the origin—the composition of juvenile sulfur.

In Fig. 5, we further test this hypothesis by comparing the deviation of data from the mass-independent array defined by $\Delta^{33}S_{sulfide}+\Delta^{36}S_{sulfide}$ with an inferred value for magnitude of the fractionation between sulfate and sulfide ($\delta^{34}S_{sulfate}-\delta^{34}S_{sulfide}$). The term $\Delta^{33}S_{sulfide}+\Delta^{36}S_{sulfide}$ takes advantage of a feature of mass-dependent fractionations and mixing whereby small $\Delta^{33}S$ variations accompany significantly larger $\Delta^{36}S$ and $\delta^{34}S$ variations. Thus the combined magnitude of mass-independent measures accentuated differences between samples. These model mixing calculations yield a similar result to the ones described by Fig. 3. Pyrites formed by mixing processes involving equilibrium isotope effects or microbial disproportionation (Fig. 5a, b) show a minimal or slight positive deviation for the quantity $\Delta^{33}S_{sulfide}+\Delta^{36}S_{sulfide}$ and produce results that are inconsistent with the field defined by the data. On the other hand, mixtures of sulfide formed by microbial sulfate reduction as predicted from laboratory culture experiments overlap with the field defined by the North Pole data.

A theoretical reaction network model (Farquhar et al., 2007b) and experimental data for microbial sulfate reduction (Johnston et al., 2007) are plotted in Fig. 5c. This shows a data-model mismatch, but both the model and observations from culture experiments indicate that microbial sulfate reduction yields pyrite with a *near zero to negative* deviation from the mass-independent array ($\Delta^{33}S_{sulfide}+\Delta^{36}S_{sulfide}$). Sulfate reducers also induce a greater deviation from the mass-independent array as the magnitude of the fractionation between sulfate and sulfide ($\delta^{34}S_{sulfate}-\delta^{34}S_{sulfide}$) increases. The pyrites from North Pole plot in a field overlapping that produced by sulfate reducers in culture experiments (Fig. 5d), lending further support to the hypothesis the Archean fractionations were produced by sulfate reducers.

In the treatment used to construct Fig. 5, we assumed that the Archean mass-independent fractionation array is best described by $\Delta^{36}S\approx-\Delta^{33}S$, and this defines the plot ordinates in Fig. 5 (as $\Delta^{33}S+\Delta^{36}S$). In Fig. 6 we undertake a similar test using the regression line through the North Pole data described by the equation $\Delta^{36}S=-1.51\cdot\Delta^{33}S-0.64$. Despite this, the data remain consistent with the field indicative of microbial sulfate reduction, including the two most negative $\Delta^{33}S$ and $\delta^{34}S$ values (Fig. 6). If this array applies (but see discussion related to Fig. 4), some of the data may reflect two-component mixing (cf. Fig. 5a) rather than simple one-step fractionations from microbial sulfate reduction alone, but if so, such mixing must still have involved sulfide produced by sulfate reducing microbes.

On the basis of this analysis, we conclude that the distribution of quadruple sulfur isotope data from North Pole is consistent with the operation of microbial sulfate reduction following mass-independent fractionation, and cannot be explained by either equilibrium hydrothermal fractionation (cf. Runnegar et al., 2001) or microbial sulfur disproportionation (cf. Philippot et al., 2007) acting alone. This conclusion holds regardless of which array is used to define the contribution from mass-independent fractionations, presuming only a constant (or nearly constant) relationship between $\delta^{34}S$, $\Delta^{33}S$ and $\Delta^{36}S$ for the mass-independent precursor reaction. We emphasize that our findings do not rule out the possible contribution of processes such as microbial disproportionation or hydrothermal fractionation to the sulfur isotope compositions of these pyrites, but if they occurred, their contribution to the mixture was minor compared to microbial sulfate reduction.

6. Conclusions

Our data from North Pole are consistent with two possibilities: (1) a highly variable mass-independent signature in which $\delta^{34}S$, $\Delta^{33}S$ and $\Delta^{36}S$ vary independently and produced by a fractionation mechanism

heretofore unknown, or (2) a mass-independent signature characterized by small variations in $\delta^{34}S$ and co-variation of $\Delta^{33}S$ and $\Delta^{36}S$ by $\delta^{34}S$, $\Delta^{36}S=-\Delta^{33}S$ that has been overprinted by a mass-dependent process that produces variations in $\delta^{34}S$, $\Delta^{33}S$ and $\Delta^{36}S$ similar to those reported from culture experiments with sulfate reducers. Our data therefore support previous suggestions for the early Archean evolution of the biological sulfate reduction pathway (Shen et al., 2001), but do not support abiological hydrothermal fractionation (cf. Runnegar et al., 2001) or microbial sulfur disproportionation (cf. Philippot et al., 2007). This conclusion holds regardless of which array is used to define the contribution from mass-independent fractionations, presuming only a constant (or nearly constant) relationship between $\delta^{34}S$, $\Delta^{33}S$ and $\Delta^{36}S$ for the mass-independent precursor reactions.

There are several possible reasons for the differences between our observations and those of Philippot et al. (2007). Their study used a different analytical method which targeted individual sulfide grains rather than bulk rock. Also, they identified only one sample with disseminated sulfides having positive $\Delta^{33}S$ and negative $\delta^{34}S$, which they argued for a signature of disproportionation. However, this signature is not ubiquitous and does not occur in bulk sulfide analyses (even for the sample with positive $\Delta^{33}S$ and negative $\delta^{34}S$). Our study speaks only to the origin of sulfur with negative $\Delta^{33}S$ and negative $\delta^{34}S$ because we did not find any samples with positive $\Delta^{33}S$ and negative $\delta^{34}S$. Hence our data do not indicate either the presence or absence of microbial sulfur disproportionation, but if this metabolism were indeed active, then its contribution to the total sulfide pool was insignificant compared to that of microbial sulfate reduction.

In closing, it should be noted that, during final corrections to this paper, Ueno et al. (2008) published similar results to ours, using similar methods from similar samples and drawing similar conclusions, albeit via somewhat different logic. Thus we contend that a strong case can now be made for the Archean evolution of microbial sulfate reduction, the earliest specific metabolic pathway identified from the geological record. This implies that essentially modern biochemical capabilities were present in micro-organisms within the first billion years of Earth's history.

Acknowledgements

This study was supported by the Canada Research Chairs program, NSERC (Y.S.), NASA #NNX07AK13G, NSF #EAR0348382, and the Guggenheim Fellowship (J.F.), and the NASA Astrobiology Institute (J.F. & R.B.). We thank two anonymous reviewers for constructive comments, and Pascal Philippot for three samples used in our study.

References

Bao, H., Rumble III, D., Lowe, D.R., 2007. The five stable isotope compositions of the fig tree barites: Implications on sulfur cycle in an early Archean ocean. Geochim. Cosmochim. Acta 71, 4868–4879.

Bekker, A., Holland, H.D., Wang, P.L., Rumble III, D., Stein, H.J., Hannah, J.L., Coetzee, L.L., Beukes, N.J., 2004. Dating the rise of the atmospheric oxygen. Nature 427, 117–120.

Berner, R.A., 1984. Sedimentary pyrite formation: an update. Geochim. Cosmochim. Acta 48, 605–615.

Blount, C.W., Dickson, F.W., 1973. Gypsum–anhydrite equilibria in systems $CaSO_4$-H_2O and $CaSO_4$-NaCl-H_2O. Am. Mineral. 58, 323–331.

Bolliger, C., Schroth, M.H., Bernasconi, S.M., Kleikemper, J., Zeyer, J., 2001. Sulfur isotope fractionation during microbial sulfate reduction by toluene-degrading bacteria. Geochim. Cosmochim. Acta 65, 3289–3298.

Buick, R., Barnes, K.R., 1984. Cherts in the Warrawoona Group: early Archaean silicified sediments deposited in shallow water environments. Univ. West. Aust. Geol. Dept Univ. Extension Spec. Publ. 9, 37–53.

Buick, R., Dunlop, J.S.R., 1990. Evaporite sediments of early Archaean age from the Warrawoona Group, North Pole, Western Australia. Sedimentology 37, 247–277.

Canfield, D.E., 2001. Biogeochemistry of sulfur isotopes. Rev. Mineral. Geochem. 43, 607–636.

Canfield, D.E., Teske, A., 1996. Late Proterozoic rise in atmospheric oxygen concentration inferred from phylogenetic and sulphur-isotope studies. Nature 382, 127–132.

Canfield, D.E., Raiswell, R., Westrich, J.T., Reaves, C.M., Berner, R.A., 1986. The use of chromium reduction in the analysis of reduced inorganic sulfur in sediments and shales. Chem. Geol. 54, 149–155.

Chambers, L.A., Trudinger, P.A., 1979. Microbiological fractionation of stable sulfur isotopes: a review and critique. Geomicrobiol. J. 1, 249–293.

Detmers, J., Brüchert, V., Habicht, K.S., Kuever, J., 2001. Diversity of sulfur isotope fractionation by sulfate-reducing prokaryotes. Appl. Environ. Microbiol. 67, 888–894.

Dunlop, J.S.R., Buick, R., 1981. Archaean epiclastic sediments derived from mafic volcanics, North Pole, Pilbara Block, Western Australia. Spec. Publs. Geol. Soc. Aust. 7, 225–233.

Farquhar, J., Wing, B.A., 2003. Multiple sulfur isotopes and the evolution of the atmosphere. Earth Planet. Sci. Letts. 213, 1–13.

Farquhar, J., Bao, H., Thiemens, M.H., 2000. Atmospheric influence of Earth's earliest sulfur cycle. Science 289, 756–758.

Farquhar, J., Savarino, J., Airieau, S., Thiemens, M.H., 2001. Observation of wavelength-sensitive mass-independent sulfur isotope effects during SO_2 photolysis: implications for the early atmosphere. J. Geophy. Res. 106, 32829–32839.

Farquhar, J., Wing, B.A., McKeegan, K.D., Harris, J.W., Cartigny, P., Thiemens, M.H., 2002. Mass-independent sulfur of inclusions in diamond and sulfur recycling on early Earth. Science 298, 2369–2372.

Farquhar, J., Johnston, D.T., Wing, B.A., Habicht, K.S., Canfield, D.E., Airieau, S.A., Thiemens, M.H., 2003. Multiple sulfur isotopic interpretations of biosynthetic pathways: implications for biological signatures in the sulfur isotope record. Geobiology 1, 27–36.

Farquhar, J., Peters, M., Johnston, D.T., Strauss, H., Masterson, A., Wiechert, U., Kaufman, A.J., 2007a. Isotopic evidence for Mesoarchaean anoxia and changing atmospheric sulphur chemistry. Nature 449, 706–708.

Farquhar, J., Johnston, D.T., Wing, B.A., 2007b. Implications of conservation of mass effects on mass-dependent isotopic fractionation: influence of network structure on sulfur isotope phase space of dissimilatory sulfate reduction. Geochim. Cosmochim. Acta 71, 5862–5875.

Farquhar, J., Canfield, D.E., Masterson, A.J., Bao, H., Johnston, D.T., 2008. Sulfur and oxygen isotope study of sulfate reduction in experiments with natural populations from Fællestrand, Denmark. Geochim. Cosmochim. Acta 72, 2805–2821.

Fike, D.A., Gammon, C.L., Ziebis, W., Orphan, V.J., 2008. Micron-scale mapping of sulfur cycling across the oxycline of a cyanobacterial mat: a paired nanoSIMS and CARD-FISH approach. ISME J. 2, 749–759.

Forrest, J., Newman, L., 1977. AG-110 microgram sulfate analysis for short time resolution of ambient levels of sulfur aerosol. Anal. Chem. 49, 1579–1584.

Groves, D.I., Dunlop, J.S.R., Buick, R., 1981. An early habitat of life. Sci. Am. 245, 64–73.

Habicht, K., Canfield, D.E., 1997. Sulfur isotope fractionation during bacterial sulfate reduction in organic-rich sediments. Geochim. Cosmochim. Acta 61, 5351–5361.

Hardie, L.A., 1967. The gypsum–anhydrite equilibrium at 1 atmosphere pressure. Am. Mineral. 52, 171–200.

Johnston, D.T., Farquhar, J., Wing, B.A., Kauf man, A.J., Canfield, D.E., Habicht, K.S., 2005a. Multiple sulfur isotope fractionations in biological systems: a case study with sulfate reducers and sulfur disproportionators. Am. J. Sci. 305, 645–660.

Johnston, D.T., Wing, B.A., Farquhar, J., Kaufman, A.J., Strauss, H., Lyons, T.W., Kah, L.C., Canfield, D.E., 2005b. Active microbial sulfur disproportionation in the Mesoproterozoic. Science 310, 1477–1479.

Johnston, D.T., Poulton, S.W., Fralick, P.W., Wing, B.A., Canfield, D.E., Farquhar, J., 2006. Evolution of the oceanic sulfur cycle at the end of the Paleoproterozoic. Geochim. Cosmochim. Acta 70, 5723–5739.

Johnston, D.T., Farquhar, J., Canfield, D.E., 2007. Sulfur isotope insights into microbial sulfate reduction: when microbes meet models. Geochim. Cosmochim. Acta 71, 3929–3947.

Kamber, B.S., Whitehouse, M.J., 2007. Micro-scale sulphur isotope evidence for sulphur cycling in the late Archean shallow ocean. Geobiology 5, 5–17.

Kaufman, A.J., Johnston, D.T., Farquhar, J., Masterson, A.L., Lyons, T.W., Bates, S., Anbar, A.D., Arnold, G.L., Garvin, J., Buick, R., 2007. Late Archean biospheric oxygenation and atmospheric evolution. Science 317, 1900–1903.

Lambert, I.B., Donnelly, T.H., Dunlop, J.S.R., Groves, D.I., 1978. Stable isotopic compositions of early Archaean sulphate deposits of probable evaporitic and volcanogenic origins. Nature 276, 808–811.

Mojzsis, S.J., 2006. Microbial sulfate reduction, multiple sulfur isotopes, and the ca. 3.46 Ga Dresser Formation (Western Australia). Trans.—Am. Geophys. Union 87 (52) Fall Meet. Suppl., Abstract V21D-07.

Mojzsis, S.J., Coath, C.D., Greenwood, J.P., McKeegan, K.D., Harrison, T.M., 2003. Mass-independent isotope effects in Archean (2.5–3.8 Ga) sedimentary sulfides determined by ion microprobe multicollection. Geochim. Cosmochim. Acta 67, 1635–1658.

Nijman, W., de Bruijne, K.H., Valkering, M.E., 1998. Growth fault control of early Archaean cherts, barite mounds and chert-barite veins, North Pole Dome, eastern Pilbara, Western Australia. Precambrian Res. 88, 25–52.

Ohmoto, H., Watanabe, Y., Ikemi, H., Poulson, S.R., Taylor, B.E., 2006. Sulphur isotope evidence for an oxic Archaean atmosphere. Nature 442, 908–911.

Ono, S., Eigenbrode, J.L., Pavlov, A., Kharecha, P., Rumble III, D., Kasting, J.F., Freeman, K. H., 2003. New insights into the Archean sulfur cycle from mass-independent sulfur isotope records. Earth Planet. Sci. Lett. 213, 15–30.

Ono, S., Wing, B.A., Johnston, D., Farquhar, J., Rumble, D., 2006. Mass-dependent fractionation of quadruple stable sulfur isotope system as a new tracer of sulfur biogeochemical cycles. Geochim. Cosmochim. Acta 70, 2238–2252.

Otake, T., Lasaga, A.C., Ohmoto, H., 2008. Ab initio calculations for equilibrium fractionations in multiple sulfur isotope systems. Chem. Geol. 249, 357–376.

Papineau, D., Mojzsis, S.J., Schmitt, A.K., 2007. Multiple sulfur isotopes from Paleoproterozoic Huronian interglacial sediments and the rise of atmospheric oxygen. Earth Planet. Sci. Lett. 255, 188–212.

Philippot, P., van Zuilen, M., Lepot, K., Thomazo, C., Farquhar, J., v an Kranendonk, M.J., 2007. Early Archean microorganisms preferred elemental sulfur, not sulfate. Science 317, 1534–1537.

Postgate, J.R., 1984. The Sulfate-reducing Bacteria, 2nd ed. Cambridge Univ. Press, Cambridge, pp. 1–208.

Rickard, D., 1997. Kinetics of pyrite formation by the H_2S oxidation of Fe(II) monosulfide in aqueous solutions between 25 °C and 125 °C: the rate equation. Geochim. Cosmochim. Acta 61, 115–134.

Runnegar, B., 2000. Archean sulfates from Western Australia: implications for the composition of Earth's early atmosphere and ocean. Eos, Trans.—Am. Geophys. Union 81 (48) Fall Meeting Supp., Abstract OS72F-12.

Runnegar, B., Dollase, W.A., Ketcham, R.A., Colbert, M., Carlson, W.D., 2001. Early Archean sulfates from Western Australia first formed as hydrothermal barites not gypsum evaporates. Geol. Soc. Am. Abstr. Prog. 33 (6), 404.

Rye, R.O., 2005. A review of the stable-isotope geochemistry of sulphate minerals in selected igneous environments and related hydrothermal systems. Chem. Geol. 215, 5–36.

Schidlowski, M., Hayes, J.M., Kaplan, I.R., 1983. Isotopic inferences of ancient biochemistries—carbon, sulfur, hydrogen, and nitrogen. In: Schopf, J.W. (Ed.), Earth's Earliest Biosphere: Its Origin and Evolution. Princeton Univ. Press, Princeton, NJ, pp. 149–186.

Shen, Y., Buick, R., 2004. The antiquity of microbial sulfate reduction. Earth-Sci. Rev. 64, 243–272.

Shen, Y., Buick, R., Canfield, D.E., 2001. Isotopic evidence for microbial sulphate reduction in the early Archaean era. Nature 410, 77–81.

Steno, N. 1669. Nicolai Stenonis de solido intra solidvm natvraliter contento dissertationis prodromus ad serenissivm Ferdinandvm II. Florentiæ: Ex typographia sub signo Stellæ, 78 pp.

Ueno, Y., Rumble, D., Ono, S., 2006. Quadruple sulfur isotope constraints on the origin of the early Archean barite and pyrite. Goldschmidt Conference Abstracts, pp. A–679.

Ueno, Y., Ono, S., Rumble, D., Maruyama, S., 2008. Quadruple sulfur isotopic analysis of ca. 3.5 Ga Dresser Formation: new evidence for microbial sulfate reduction in the early Archean. Geochim. Cosmochim. Acta 72, 5675–5691.

van Kranendonk, M.J., 2006. Volcanic degassing, hydrothermal circulation and the flourishing of early life on Earth: a review of the evidence from c.3490–3240 Ma rocks of the Pilbara Supergroup, Pilbara Craton, Western Australia. Earth-Sci. Rev. 74, 197–240.

Wilkin, R.T., Barnes, H.L., 1996. Pyrite formation by reactions of iron monosulfides with dissolved inorganic and organic sulfur species. Geochim. Cosmochim. Acta 60, 4167–4179.